



Parametric investigation for suppressing near-field thermal radiation between two spherical nanoparticles[☆]

Y. Zhao, G.H. Tang^{*}, Z.Y. Li

MOE Key Laboratory of Thermo-Fluid Science and Engineering, School of Energy and Power Engineering, Xi'an Jiaotong University, Xi'an 710049, China

ARTICLE INFO

Available online 24 May 2012

Keywords:

Near-field radiation
Nanoparticle
Dielectric function
Si-doped

ABSTRACT

The research on the near-field thermal radiation between two nanoparticles separated by nanoscale distance is of great significance and is closely related with the materials design. The remarkably increased radiation energy transfer may be harmful to the performance of super-insulating materials such as silica aerogels with nanoporous structures. Based on the fluctuation–dissipation theorem, this article analytically investigates the influences of important parameters including the distance, particle radius, dielectric function and doping levels on the near-field heat transfer between two spherical nanoparticles. By tuning these parameters, it is expected to control the near-field thermal radiation. This study will help in investigating the heat transfer of group nanoparticles and developing novel insulating materials with special properties.

© 2012 Elsevier Ltd. All rights reserved.

1. Introduction

When the distance between two nanoparticles becomes less than the mean free path or the characteristic wavelength of thermal radiation, the radiation heat transfer will no longer be independent of the distance but has a relationship with that. The interference effect and photon tunneling effect in this scale are particularly remarkable. When the coherence length of thermal radiation reaches the same order of magnitude as the characteristic wavelength, the waves of thermal radiation present coherence, leading to the radiation heat transfer characteristics and radiative heat flux fluctuating with the distance, which is usually called the interference effect. Photon tunneling effect is due to the existence of evanescent waves near the surface of the object. The interaction of those evanescent waves will increase the radiation heat transfer between two objects. Narayanaswamy et al. [1] has experimentally proved that the near-field radiative heat transfer could exceed the one between two black bodies by several orders of magnitude. The purpose of this research is to investigate the suppression of such an increased radiative heat transfer to meet some particular applications.

Super-insulating materials such as aerogels with nanoporous structures usually involve heat transfer between neighboring particles. These materials are essentially made of a nanoporous matrix of amorphous silica nanoparticles (more than 90% of the solid volume fraction) which contributes most to thermal properties of these super-insulating materials [2]. Such particles and pores of the aerogel are very small: the pure aerogel has an average particle diameter

between 2 and 5 nm and the pore diameter between 10 and 100 nm [3]. Such a nanoscale may cause the near-field radiation, and then the remarkably increased energy transfer will be harmful to the performance of the insulation materials. It is therefore critical to figure out the energy transfer mechanism in nanoscale. Since the radiative properties of super-insulating materials in nanostructure are quite complicated and difficult to research, we take the basic unit of porous media – the nanoparticle as our investigation object. Though the basic principle of near-field radiation between two particles was introduced [4–8], the parameters for suppressing the near-field radiation have not been involved. What interests us is how to get insulation materials with high performance by adjusting parameters to suppress the near-field energy transfer at most. Compared to few studies on suppressing near-field radiative transfer, there are some studies that have been conducted on increasing the nanoscale radiative transfer in some specific applications, such as thermophotovoltaic devices. Basu and his colleagues [9–11] investigated the maximum achievable radiative heat flux between two parallel plates and obtained optimal parameters in the dielectric functions and suitable film thicknesses for maximizing near-field heat transfer between two parallel plates. Though it seems that suppressing the energy transfer is a simple reverse process to increasing the energy transfer, there are some special issues to be discussed, for example: How to control the peak values, widths and locations of spectral heat flux and so on. In this research, a parametric study is performed to investigate the effect of different parameters on near-field heat transfer based on the fluctuation–dissipation theorem. Characteristics and influence of these parameters are obtained which can suppress nanoscale radiative heat transfer between two spherical nanoparticles separated by the vacuum gap on the order of tens of nanometers.

[☆] Communicated by: P. Cheng and W.Q. Tao.

^{*} Corresponding author.

E-mail address: ghtang@mail.xjtu.edu.cn (G.H. Tang).

Nomenclature

a	nanoparticle radius (nm)
d	center distance between two spherical nanoparticles (nm)
\hbar	Planck's constant over 2π
k_B	Boltzmann's constant
k	radiative heat transfer coefficient (W/K)
m^*	carrier effective mass (kg)
m_e	free-electron mass in vacuum (kg)
N	carrier concentration (cm^{-3})
T	temperature (K)

Greek symbols

α	polarisability of a spherical nanoparticle
ε_∞	limiting value of the dielectric function at high frequencies
ε_p	dielectric function
Φ	total radiative heat flux (W)
Φ_ω	spectral heat flux (W rad/s)
γ	scattering rate
λ	wave length (μm)
μ	mobility (cm^2/Vs)
τ	relaxation time (fs)
ω	angular frequency (rad/s)
θ	mean energy of Planck's oscillator (μJ)
ω_p	plasma frequency (rad/s)
ω_{Lo}	longitudinal optical phonon frequencies (rad/s)
ω_o	transverse optical phonon frequencies (rad/s)

2. Objective function and adjustable parameters

The radiative heat transfer between two spherical nanoparticles can be studied by employing the dipole approximation to spherical nanoparticles, and using the electromagnetic field theory and fluctuation–dissipation theorem. Considering that the characteristic scale is ten to one hundred nanometers and assuming that the electromagnetic field inside the particle is unchanged, the total radiative heat flux between two spherical nanoparticles at temperatures T_1 and T_2 , separated by a center distance d , is given by [12]

$$\Phi = \int_0^\infty \frac{3\text{Im}[\alpha_1(\omega)]\text{Im}[\alpha_2(\omega)]}{4\pi^3 d^6} [\theta(\omega, T_1) - \theta(\omega, T_2)] d\omega. \quad (1)$$

In the above equation, ω is the angular frequency and $\theta(\omega, T) = \hbar\omega / [\exp(\hbar\omega/k_B T) - 1]$ is the mean energy of Planck's oscillator, where $\hbar = h/2\pi$ is the Planck's constant over 2π and k_B is the Boltzmann's constant. $\alpha(\omega)$ is the polarisability of a spherical nanoparticle of radius a . Assuming that $\alpha(\omega)$ satisfies the Coffin–Manson relationship [13], which can be expressed as

$$\alpha(\omega) = 4\pi a^3 \frac{\varepsilon_p(\omega) - 1}{\varepsilon_p(\omega) + 2}, \quad (2)$$

where $\varepsilon_p(\omega)$ represents the dielectric function of particle, which can be described by either the Drude model or Lorentz model.

This study aims at suppressing the near-field radiative heat transfer between two spherical nanoparticles and thus Eq. (1) is the objective function. We can see from Eq. (1) that the spatial dependence is expressed in the form of $1/d^6$. This dependence is typical of the dipole–dipole interaction. That is considered as a Van der Waals force, in the literature [14], interpreted in the

following way. The fluctuations (thermal or quantum fluctuations) distort the charge distribution of a nanoparticle and produce a fluctuating dipole. This fluctuating dipole induces in turn an electromagnetic field on the other nanoparticle initiating a second dipole. This dipole interaction causes both an energy transfer and a momentum transfer or force. For molecules, this energy transfer is known as Forster transfer and the force is called Van der Waals force. Nanoparticles follow a similar behavior with a resonance at the surface polariton resonance. Eq. (1) also shows that the radiation energy transfer rate between two particles depends on the imaginary part of the polarization. It is obvious that the polarisability has a resonance when the dielectric constant approaches to the value of -2 provided that the imaginary part of the dielectric constant is not too high. The particle resonance occurs in the visible regime of the spectrum for metals and in the infrared regime for polar materials.

In order to keep the electromagnetic field inside the particle unchanged, the near-field radiation is calculated under the condition of $d > 5(a_1 + a_2)$.

3. Results and discussion

In this section, the influences of the distance, particle radius, temperature, dielectric function and doping levels on the radiation heat transfer between two spherical nanoparticles are analytically investigated. The calculated particles are SiC, which are nonmagnetic materials.

3.1. Effect of distance and particle radius

Because the distance d and particle radius a are outside the integral sign in Eq. (1), and both have nothing to do with the angular frequency, we can draw a conclusion from Eqs. (1) and (7) that the total radiative heat flux is inversely proportional to the distance to the 6th power and proportional to the particle radius to the 3rd power, when the distance between nanoparticles is very small. Note that the air in aerogels is mainly made up of nitrogen and oxygen, whose mean free path is about 70 nm. The thermal convection can be eliminated inside such insulation materials when the pore diameter is less than 50 nm. Therefore, under the elimination of convection, increasing the distance between nanoparticles can effectively reduce the near-field radiation. Eq. (1) can only be used to calculate the nanoparticle radiation in near-field, which is the theoretical limitation. To meet dipole approximation conditions, the internal electromagnetic field of particle has to be kept at the same. Thus it is required that particles cannot get too close to each other so as not to influence electromagnetic fields of their own. If the distance between two particles is equal or less than the diameter of particles, one particle's electromagnetic field distribution within the other particle cannot be regarded as uniform.

3.2. Effect of temperature

Fig. 1(a) and (b) plot Φ_ω and k at $T_2 = 1000$ K, 700 K and 400 K, when $T_1 = 300$ K. We can see that the effect of temperature is very small in Fig. 1(a). For the convenience of comparison, the radiative heat transfer coefficient k is defined as $k = \Phi / |T_1 - T_2|$ with the unit of W/K. The calculated coefficients are shown in Fig. 1(b). It can be seen that the deviations between the radiative heat transfer coefficients caused by the three temperature differences are very small. Thus we can conclude that the effect of temperature is quite less than the distance and particle radius.

From Fig. 1(a) we can see that the heat transfer in the vicinity of a particular wavelength is higher in magnitude of about a dozen orders than that in other regimes. This large energy transfer is due to the excitation of surface plasmon polaritons [15,16]. The radiation heat transfer in other wavelengths is almost zero, and this plasma

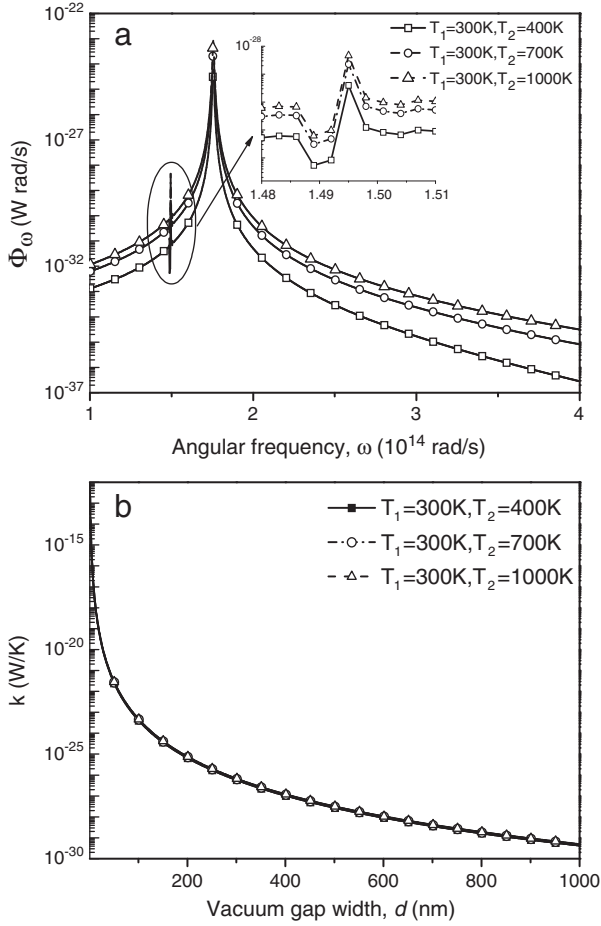


Fig. 1. Spectral heat flux and radiative heat transfer coefficient calculated at three different temperatures. (a) The spectral heat flux and (b) radiative heat transfer coefficient.

frequency depends on $\text{Im}[\varepsilon_p(\omega)]$ and $1/|\varepsilon_p(\omega) + 2|$. When the value of $\text{Im}[\varepsilon_p(\omega)]$ becomes very large or $\text{Re}[\varepsilon_p(\omega)]$ approaches to -2 under the lower value of imaginary part of the dielectric function, the two peak values occur in the curves. For the SiC material, the first plasma frequency is $\omega_1 \approx 1.494 \times 10^{14} \text{ rad/s}$ since the peak value of $\text{Im}[\varepsilon_p(\omega)]$ appears in this frequency. We can observe that the second plasma frequency is $\omega_2 \approx 1.756 \times 10^{14} \text{ rad/s}$ since at this frequency the real part of the dielectric function approaches to -2 . Therefore by adjusting the dielectric function of materials it enables that the frequency of the heat source deviates from this plasma frequency and thus the reduction of radiative heat flux could be achieved.

3.3. Effect of dielectric function

In this section, a parametric study is performed to investigate the effect of different parameters in dielectric function models on near-field heat transfer by using the fluctuation–dissipation theorem. Both the Drude and Lorentz models on the near-field heat flux are investigated. For real materials, the parameters in the dielectric function model are temperature dependent, but few studies have been conducted on that probably because the parameters vary unpredictably with temperature changing. Therefore the parameters in the dielectric function are assumed to be independent of temperature in this study. But for doped silicon dielectric function, the impact of temperature on the dielectric function is considered.

3.3.1. The Drude model

The Drude model which describes the dielectric function of free carriers is given by [17]:

$$\varepsilon(\omega) = \varepsilon_\infty - \frac{\omega_p^2}{\omega^2 + i\omega\gamma}, \quad (3)$$

where ε_∞ is the limiting value of the dielectric function at high frequencies, γ is the scattering rate, and ω_p is the plasma frequency. In this study, ε_∞ , ω_p and γ are treated as adjustable parameters to suppress the near-field heat flux. According to Eq. (3), the real and imaginary parts of the dielectric function given by the Drude model can be expressed as

$$\varepsilon'(\omega) = \varepsilon_\infty - \frac{\omega_p^2}{\omega^2 + \gamma^2}, \quad \text{and} \quad \varepsilon''(\omega) = \frac{\gamma\omega_p^2}{\omega^3 + \omega\gamma^2}. \quad (4)$$

Based on the Drude model for materials, we derived the following expression for the imaginary parts of the polarisability of the spherical nanoparticle.

$$\begin{aligned} \text{Im}[\alpha(\omega)] &= 4\pi a^3 \text{Im} \left[\frac{\varepsilon_p(\omega) - 1}{\varepsilon_p(\omega) + 2} \right] = 12\pi a^3 \frac{\text{Im}[\varepsilon_p(\omega)]}{|\varepsilon_p(\omega) + 2|^2} \\ &= \frac{12\pi a^3 \gamma \omega_p^2}{(\omega^3 + \omega\gamma^2) \left[\left(\varepsilon_\infty - \frac{\omega_p^2}{\omega^2 + \gamma^2} + 2 \right)^2 + \left(\frac{\gamma\omega_p^2}{\omega^3 + \omega\gamma^2} \right)^2 \right]} \end{aligned} \quad (5)$$

It can be seen that increasing ε_∞ will decrease the imaginary parts of the polarisability and then reduce the heat flux. Fig. 2 presents the spectral near-field heat transfer between two particles separated by a center distance d . We can see that the scattering rate mainly determines the width of the spectral heat flux curve. From Fig. 2 the peak of the spectral heat flux decreases and broadens when the scattering rate increases. This trend of the curves is coincident with the spectral heat flux trend between two semi-infinite media [17]. Considering that it is mainly the area under the spectral heat flux curve that represents the total heat flux, an optimal value of γ can be obtained in order to suppress the energy transfer.

3.3.2. The Lorentz model

The dielectric function of many polar materials can be described by the Lorentz model [17]:

$$\varepsilon(\omega) = \varepsilon_\infty - \frac{\omega_p^2}{\omega^2 + i\omega\gamma - \omega_0^2}, \quad (6)$$

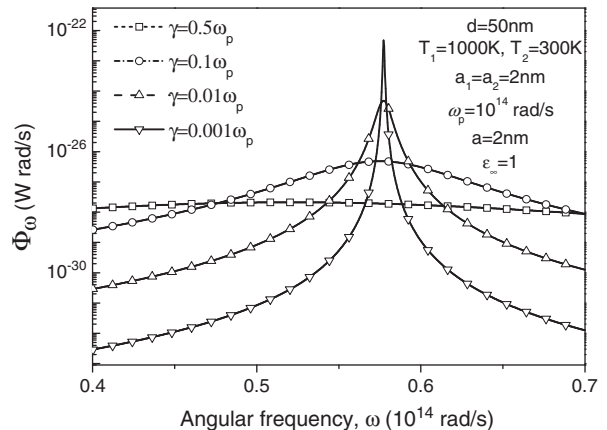


Fig. 2. The spectral heat flux for different γ .

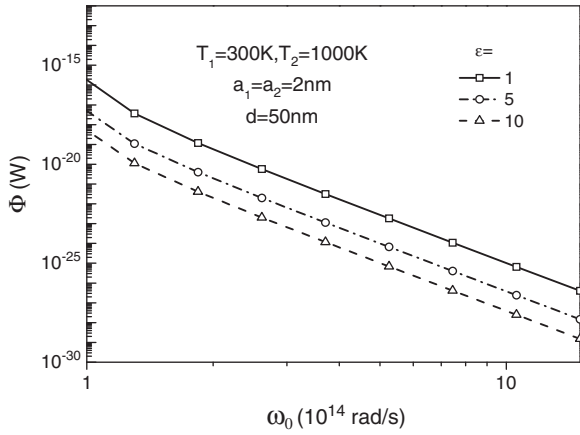


Fig. 3. Total heat flux as a function of ω_0 for different ϵ_∞ values.

where $\omega_p^2 = \epsilon_\infty(\omega_{LO}^2 - \omega_0^2)$, ω_{LO} and ω_0 are the frequencies corresponding to the longitudinal and transverse optical phonons, respectively. Note that ω_p determines the strength of the oscillators in the Lorentz mode, and when $\omega_0 = 0$, Eq. (6) reduces to Eq. (3). Hence, the Lorentz model provides an additional adjustable parameter ω_0 compared to the Drude model. The heat fluxes as a function of ω_0 for $\epsilon_\infty = 1, 5$ and 10 are plotted in Fig. 3. The heat flux is decreasing with increasing ω_0 . In addition, larger value of ϵ_∞ in the Lorentz model will also decrease the near-field radiation.

3.4. Effect of Si-doped

Doped nanoparticle is very interesting because its dielectric function can be tuned by modifying the carrier concentration N . In this section we take the doped Si as an example. In order to analyze the nanoscale thermal radiation for doped-Si, it is important to first understand the optical properties of Si at different doping levels. Due to the large number of free carriers in doped-Si, the Drude model can be applied to determine its dielectric function in the infrared region. For doped silicon in the infrared region, the Drude model is given as

$$\epsilon(\omega) = \epsilon_\infty - \frac{\omega_p^2}{\omega(\omega + i/\tau)} \tag{7}$$

In the infrared domain ($\lambda > 2\mu\text{m}$), ϵ_∞ may be considered as a constant equal to 11.7 [18]. The plasma frequency and the scattering time can be expressed as $\omega_p^2 = Ne^2/(m^*\epsilon_0)$ and $\tau = m^*\mu/e$, respectively,

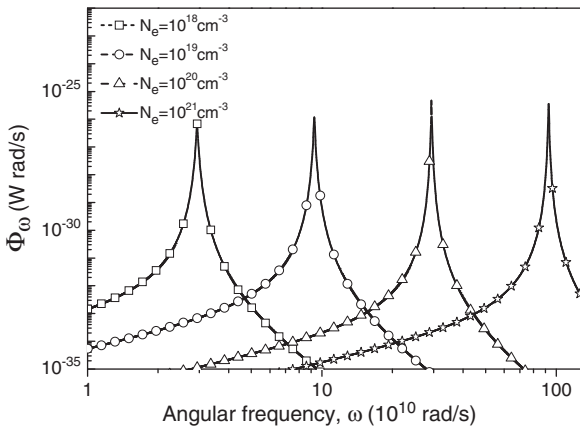


Fig. 4. The spectral heat flux for different doping concentrations.

where ϵ_0 is the permittivity of free space, e is the electron charge, N is the carrier concentration, m^* is the carrier effective mass, and μ is the mobility. For heavily doped silicon, the effective mass depends little on the temperature, doping concentration, or frequency. Hence, the effective mass of electron for the n-doped silicon and hole for the p-doped silicon can be taken as $0.27m_e$ and $0.37m_e$, respectively, where m_e is the free-electron mass in vacuum [19]. Only n-doped Si is considered in this study since the results for p-doped Si would be similar. For impurity scattering, the temperature-dependent mobility is given as $\mu(T) = \mu_{300}(T/300)^{1.5}$ [20], where the subscript 300 denotes the value at 300 K. The value of μ_{300} for n-doped Si can be obtained [21]

$$\mu_{300} = \mu_1 + \frac{\mu_{\max} - \mu_1}{1 + (N_e/C_r)^\alpha} - \frac{\mu_2}{1 + (C_s/N_e)^\beta} \tag{8}$$

Here, $\mu_1 = 68.5 \text{ cm}^2/\text{Vs}$, $\mu_{\max} = 1414 \text{ cm}^2/\text{Vs}$, $\mu_2 = 56.1 \text{ cm}^2/\text{Vs}$, $C_r = 9.2 \times 10^{16} \text{ cm}^{-3}$, $C_s = 3.41 \times 10^{20} \text{ cm}^{-3}$, $\alpha = 0.711$, $\beta = 1.98$, and N_e is the electron concentration [21].

A remarkable property in doped nanoparticles is that the peak of the spectral heat flux can be shifted by modifying the density of electrons. This can be easily done by changing the level of doping. Eq. (1) is plotted against ω for three different doping concentrations in Fig. 4 for $T_1 = 1000 \text{ K}$ and $T_2 = 300 \text{ K}$. It can be seen that the location of the peak in Φ_ω depends on the concentration and shifts toward higher frequencies with increased doping level. Compared to tuning peaks and widths of the spectral heat flux in Fig. 2, this displacement shows that it is possible to suppress the heat transfer by varying N to avoid the peak of the spectral heat flux when building nanoporous insulating materials.

4. Conclusions

The effects of distance, particle radius, parameters in the Drude and Lorentz models, and the Si-doped on near-field radiation between two nanoparticles are investigated by using the fluctuation-dissipation theorem. And the values of parameters that suppress the near-field heat transfer are determined. It is observed that larger distance between two particles and smaller diameter of particles can decrease the near-field radiation. The effect of temperature is much less than the distance and particle radius. For the Drude model, the optimal value of γ can be obtained from actual conditions for minimum radiative transfer. For both applied models, the near-field radiation decreases with larger ϵ_∞ . In the Lorentz model, the near-field heat flux monotonically decreases with increasing ω_0 at a fixed ϵ_∞ . For the Si-doped, the doping concentration can determine the peak location of Φ_ω , and by changing N it is possible to avoid the peak of the spectral heat flux so as to suppress the heat transfer. The results from this study will be helpful to investigate the heat transfer of group nanoparticles and develop novel insulating materials with particular properties.

Acknowledgment

This work was supported by the National Natural Science Foundation of China under Grant No. 51076125.

References

- [1] A. Narayanaswamy, S. Shen, L. Hu, X.Y. Chen, G. Chen, Breakdown of the Planck blackbody radiation law at nanoscale gaps, Applied Physics A 96 (2009) 357–362.
- [2] S. Lallich, F. Enguehard, Experimental determination and modeling of the radiative properties of silica nanoporous, ASME Journal of Heat Transfer 131 (2009) 082701.
- [3] S.Q. Zeng, A.J. Hunt, W. Cao, R. Greif, Pore size distribution and apparent thermal conductivity of silica aerogel, ASME Journal of Heat Transfer 116 (1994) 756–759.

- [4] G. Domingues, S. Volz, K. Joulain, J.J. Greffet, Heat transfer between two nanoparticles through near field interaction, *Physical Review Letters* 94 (2005) 085901.
- [5] P.O. Chapuis, M. Laroche, S. Volz, J.J. Greffet, Radiative heat transfer between metallic nanoparticles, *Applied Physics Letters* 92 (2008) 201906.
- [6] A. Pérez-Madrid, J.M. Rubi, L.C. Lapas, Heat transfer between nanoparticles: thermal conductance for near-field interactions, *Physical Review B* 77 (2008) 155417.
- [7] A. Pérez-Madrid, L.C. Lapas, J.M. Rubi, Heat exchange between two interacting nanoparticles beyond the fluctuation–dissipation regime, *Physical Review Letters* 103 (2009) 048301.
- [8] A. Narayanaswamy, G. Chen, Thermal near-field radiative transfer between two spheres, *Physical Review B* 77 (2009) 075125.
- [9] S. Basu, Z.M. Zhang, Review of near-field thermal radiation and its application to energy conversion, *International Journal of Energy Research* 33 (2009) 1203–1232.
- [10] X.J. Wang, S. Basu, Z.M. Zhang, Parametric optimization of dielectric functions for maximizing nanoscale radiative, *Journal of Physics D: Applied Physics* 42 (2009) 245403.
- [11] S. Basu, M. Francoeur, Maximum near-field radiative heat transfer between thin films, *Applied Physics Letters* 98 (2011) 243120.
- [12] S. Volz, *Microscale and Nanoscale Heat Transfer*, Springer Berlin Heidelberg, New York, 2007.
- [13] J.D. Jackson, *Classical Electrodynamics*, American Association of Physics Teachers, New York, 1998.
- [14] K. Joulain, J.P. Mulet, F. Marquier, R. Carminati, J.J. Greffet, Surface electromagnetic waves thermally excited: radiative heat transfer, coherence properties and Casimir forces revisited in the near field, *Surface Science* 57 (2005) 59–112.
- [15] A.I. Volokitin, B.N.J. Persson, Resonant photon tunneling enhancement of the radiative heat transfer, *Physical Review B* 69 (2004) 045417.
- [16] J.P. Mulet, K. Joulain, R. Carminati, J.J. Greffet, Enhanced radiative heat transfer at nanometric distances, *Nanoscale and Microscale Thermophysical Engineering* 6 (2002) 209–222.
- [17] X.J. Wang, S. Basu, Z.M. Zhang, Parametric optimization of dielectric functions for maximizing nanoscale radiative transfer, *Journal of Physics D: Applied Physics* 42 (2009) 245403.
- [18] C.J. Fu, Z.M. Zhang, Nanoscale radiation heat transfer for silicon at different doping levels, *International Journal of Heat and Mass Transfer* 49 (2006) 1703–1718.
- [19] N.W. Ashcroft, N.D. Mermin, *Solid State Physics*, Saunders, Philadelphia, 1976.
- [20] S. Basu, B.J. Lee, Z.M. Zhang, Near-field radiation calculated with an improved dielectric function model for doped silicon, *ASME Journal of Heat Transfer* 132 (2010) 023302.
- [21] G. Masetti, M. Severi, S. Solmi, Modeling of carrier mobility against carrier concentration in arsenic-, phosphorus-, and boron-doped silicon, *IEEE Transactions Electron Devices* 30 (1983) 764–769.